Implementation of Lattice Kinetic Monte Carlo algorithm

Aditya Sundar,[1] Ramin Ansari,[2] and Nelson David Rufus[3]

[1] *Department of Materials Science and Engineering, University of Michigan, Ann Arbor, MI-48109*[a)]

[2] *Department of Chemical Engineering, University of Michigan, Ann Arbor, MI-48109*[b)]

[3] *Department of Mechanical Engineering, University of Michigan, Ann Arbor, MI-48109*[c)]

(Dated: 19th April, 2018)

Two and three dimensional lattice Monte Carlo models have been developed to understand crystal growth and phase stability of different structure. Growth of stoichiometric zinc blende phase GaAs is presented using rates for atom addition, surface diffusion and temperature as the external controllables. To characterize the morphology of the films, the evolution of the mean square surface roughness with temperature and time has been computed. Statistical averages indicate that the roughness decreases at higher growth temperatures since atom diffusion is enhanced. This also allows the surface to maintain lower roughness for the entire growth duration. Thereafter, Nudged Elastic Band (NEB) calculations are described and performed for application to the 3D Monte Carlo simulations. Finally, 3D Lattice Monte Carlo applications are presented with the Metropolis algorithm for equilibrium structure calculation and Kinetic Monte Carlo for diffusion of vacancy.

I. INTRODUCTION

Lattice Monte Carlo methods are a class of simulation techniques to study the evolution of a given crystal structure. Lattice Kinetic Monte Carlo methods have been employed to study crystal growth, defect dynamics etc in several metallic and non-metallic systems. These methods are usually used in conjunction with Density Functional Theory or Molecular Dynamics calculations to obtain crucial inputs for rate calculation in the Monte Carlo process. Early stages of wurtzite GaN growth along (0001) were studied recently by lattice kMC[1,2]. By including ab initio rates for different atomic rearrangement processes, morphological evolution from random clusters to ordered island formation was captured successfully by the model. Atomic deposition and surface diffusion were the considered processes while defect formation and bulk diffusion were neglected. The effect of the substrate surface ((0001) vs ($01\bar{1}0$)) wurtzite GaN growth has also been investigated[3]. Growth of rocksalt TiN along (001) has also been modeled by lattice kMC to study the formation of dense and porous microstructures under different growth environments[4].

This article is organised as follows. In section II, the 2D lattice kMC implementation is discussed. Crystal growth of GaAs (model III-V semiconductor) has been studied by simulating surface adsorption and diffusion processes. The relevant reaction rates are obtained from literature. In section III, 3D simulations are discussed. We have designed a set of NEB simulation to study vacancy diffusion in crystalline silicon. The relevant energy barriers obtained from NEB simulations are then used for 3D Lattice Monte Carlo simulations. Additionally, the equilibrium structural arrangement of GaAs is established by Metropolis Monte Carlo methods.

II. 2D LATTICE MONTE CARLO FOR CRYSTAL GROWTH

GaAs is one of the several semiconducting crystals belonging to the III-V family that is known to exist in zinc blende and wurtzite phases. Epitaxial growth of thin films, nanowires and other architectures have revealed the existence of both phases and the reasons for the observed phase transformations are still being investigated. Recently it was shown that initial stages of nanowire growth result in mixed phases (blende-wurtzite)[5]. Increasing growth duration was found to result in phase purification. Evolution of the crystallinity is also a function of the growth conditions, precursors and nature of the substrate. In this study, we simulate the homoepitaxial growth of a zinc-blende phase film on a substrate. The assumptions in this model are listed below.

(i) Fixed crystal structure. The materials is assumed to grow in the zinc blende phase for all considered temperatures. This does not capture the possibility of transformations to the wurtzite phase.

(ii) Only atom addition and surface diffusion processes are considered.

(iii) Homoepitaxial process. There is no lattice mismatch or strain at the substrate/film interface.

A. Simulation cell and algorithm

For growth along the (111) surface, the substrate is defined to contain 30 lattice sites. At each temperature, the simulation was run for a total time of $t_{total} = 0.1$ seconds. The simulation time was incremented after

---

each diffusive step according to the Residence Time Algorithm. To model growth of the crystal, a new atom (Ga or As) was added to a randomly chosen site every t_{add} seconds. In between successive addition steps, the surface species are allowed to diffuse. For a given Monte Carlo step, surface atoms at each of the 30 sites are allowed to diffuse to the site on the left and right provided there is a vacancy. The total rate $\sum r$ is obtained by summing over the rates of all possible transitions. The time step for each step is calculated as $\frac{-\mathrm{Log}(r_1)}{\sum r}$ where r_1 is a random number $\in (0, 1]$. For results discussed here t_{add} was set to 10^{-4} s. The total number of atoms added is given by $\frac{t_{total}}{t_{add}} = 1000$. The surface profile, evolution of the mean square roughness as a function of time and temperature are discussed below. At each temperature, the simulation was repeated 6 times and the averaged properties are presented here.
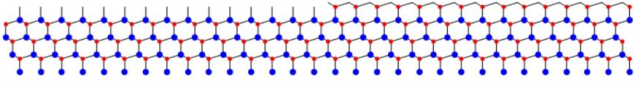

FIG. 1. Substrate showing perfectly ordered GaAs lattice. Ga and As atoms are depicted by blue and red balls circles respectively. One layer along the $< 111 >$ direction is defined as one Ga-As pair.

Projection of 3D zinc blende lattice on a plane
Each atom in the zinc blende structure is tetrahedrally bonded to 4 atoms of the other species. These are 4 nearest neighbours at the NN1 position. The next nearest neighbours of an atom are the 12 NN2 neighbours on the same FCC lattice. The planar 2D representation has reduced number of NN1 and NN2 sites since there is a projection overlap. Consequently, only 3 of the 4 NN1 positions and 6 of the 12 NN2 positions are visible.

B. Reaction rates

The reaction rate for each surface diffusion step is calculated by using the Arrhenius expression.

$$r = \nu \exp\left(-\frac{E_b}{kT}\right) = \nu \exp\left(-\frac{E_0 + \Delta E}{kT}\right) \quad (1)$$

where $\nu = 10^{13}$/s is the jump frequency, E_b is the energy barrier for the diffusive jump, $k = 1.308 \times 10^{-23}$ J/K is the Boltzmann constant and T is the temperature. $E_0 = 1.26$ eV is the base diffusion barrier and $\Delta E = E_f - E_i$ captures the local configurational energy difference between the jump sites. In this simulation, E is evaluated by counting the bond energies up to the second nearest neighbour for each site. The bond energies for the Ga-Ga, As-As and Ga-As interactions

are listed in Table .

E_{NN1}(eV)	Ga	As	E_{NN2} (eV)	Ga	As
Ga	0.3	0.5	Ga	0.15	0
As	0.5	0.1	As	0	0.05

TABLE I. First and second nearest neighbour energies[6]

$$E = \sum_{NN1} E_{NN1} + \sum_{NN2} E_{NN2} \quad (2)$$

The acceptance/rejection criteria for a transition is set as follows. If $E_f - E_i > 0$ (hop to a better coordinated site), $E_b = E_0$. If $E_f - E_i < 0$ (hop to a poorly coordinated site), $E_b = E_0 - \Delta E$. This formalism for diffusion rate calculations was borrowed from[6].

C. Results and discussion

1. Morphology evolution

Since the total number of atoms added at each temperature was constant, the average height of the films is expected to be the same (since 1000 lattice positions will be occupied). However, the surface morphology is expected to evolve with changing temperature. It is observed that the surface becomes smother at higher temperatures. From the diffusion rate equation, higher T results in faster rates and consequently the time incremented after every diffusive step is lesser. This allows for enhanced surface diffusion between atom addition steps. As a result, there is sufficient time for the surface atoms to re-organise themselves into a higher coordinated state. Graphics obtained at each temperatures are shown in Figures 2-7. The inset for each figure is from another simulation using the same parameters.
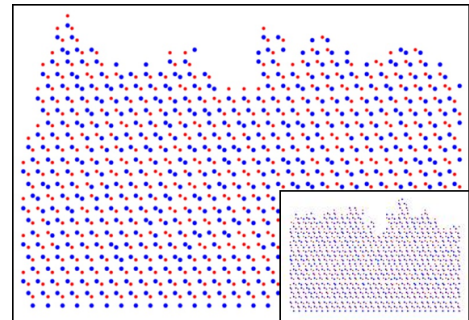

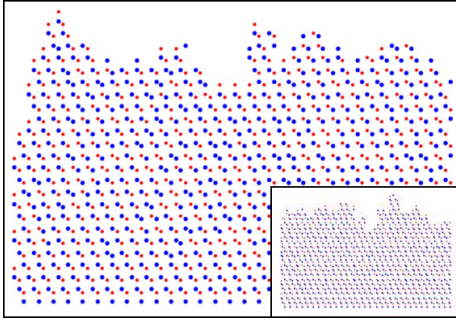FIG. 2. Surface at 1000 K after 0.1 s.

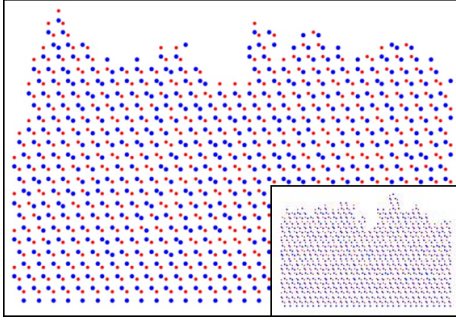FIG. 3. Surface at 1100 K after 0.1 s.

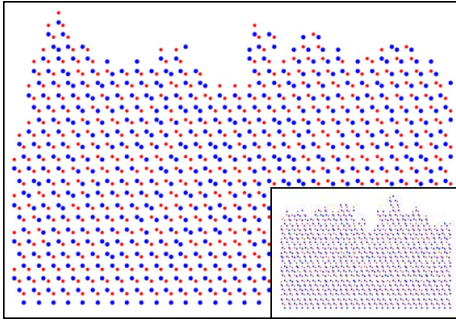FIG. 4. Surface at 1200 K after 0.1 s.
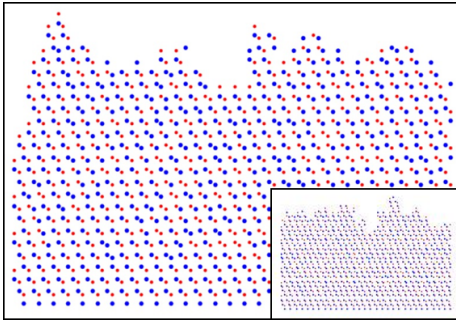

FIG. 5. Surface at 1300 K after 0.1 s.

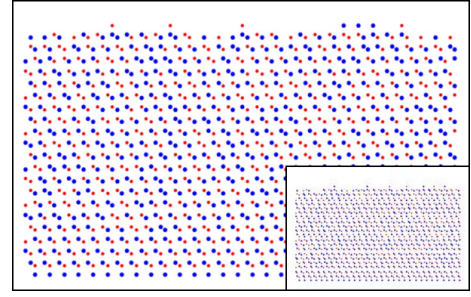FIG. 6. Surface at 1400 K after 0.1 s.

FIG. 7. Surface at 1500 K after 0.1 s.

2. Roughness evolution

The mean square roughness (MSR) of the (111) growth front was calculated after each time step increment.

$$\rho^2 = < [h(r,t) - \bar{h}(t)]^2 >$$

where ρ is the MSR, $h(r,t)$ is the height at each lattice point r at time t and $\bar{h}(t)$ is the height averaged over all lattice points at time t. These results were compared
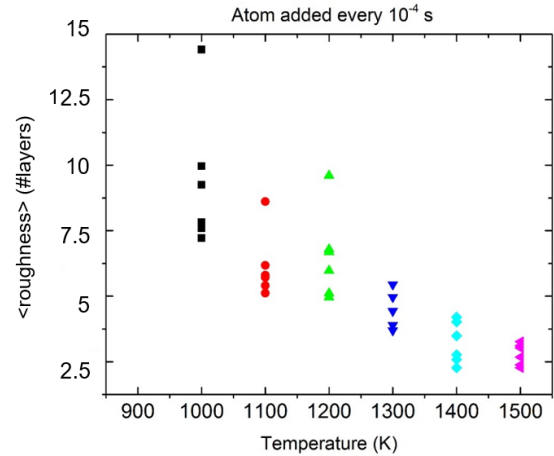

FIG. 8. The surface roughness calculated after 6 simulations at each temperature is plotted here. A nearly monotonous decrease in the MSR is observed with increasing temperature. Each layer along the (111) direction is defined as a Ga-As pair.

with previous publications to check the validity of the predicted trends. Several reports have shown the film roughness in III-V materials to reduce with increasing growth temperatures. Experimental studies using Atomic Force Microscopy[7] show the surface roughness of GaN to decrease from $\approx$ 40 nm (550°C) to $\approx$ 5 nm (880°C). InAs morphology was also shown to evolve when the temperature was increased from 900°C to 1200 °C[8]. Additionally, time evolution of roughness measured by surface reflectivity techniques also show oscillatory behaviour as computed from this kMC simulation.
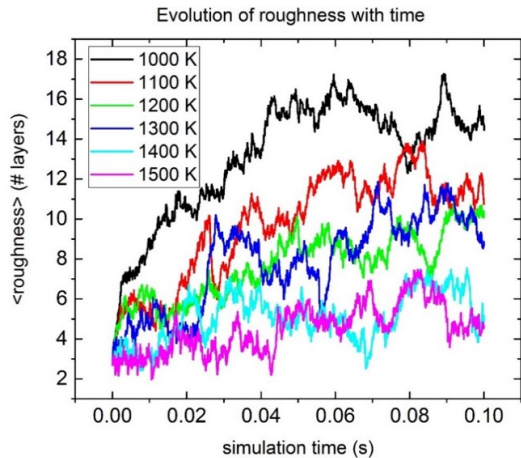
FIG. 9. The time evolution of surface MSR shows identical qualitative behaviour for all temperatures studied. The oscillatory pattern indicates the growth of successive layers. The MSR for higher growth temperature is lower throughout the entire duration of the growth process.

This simulation only accounts for ad-atom addition and diffusion on the same layer. To accurately simulate real crystal growth, other phenomena such as long range diffusion, multi-step diffusion, atom desorption also need to be accounted for. Most importantly, this model is suitable to study structure whose phase stability is known. Since this assumes a rigid lattice model, it cannot capture temperature dependent crystal structure transformations. T capture those phenomena, one needs to include the possibility of additional lattice sites and calculate the relative probabilities of each possible Monte Carlo process. Further, kMC can be interfaced with atomic pair potentials to perform non-lattice simulations. If the crystal stability of a material is not known a priori, simulations should predict phase formation and stabilities.

III. 3D LATTICE MONTE CARLO

A. Nudged Elastic Band calculations

The nudged elastic band (NEB) is a method for finding minimum energy paths between two initial and final positions. Linear interpolation from initial to final position might not be the minimum energy path. Therefore, a number of intermediate images along the reaction path have been used to optimize. Both the atomic configuration and the energy barrier associate with the transition can be investigated by this method. We performed the implementation of NEB method in LAMMPS[9] software using 8 replicas of a system. In this work, we used the Stillinger-Weber (SW) potential for

silicon. Two different systems were studied. First, we carried out a single vacancy migration in bulk and then we studied a vacancy migration with only taking the first nearest neighbors into account.

To get the vacancy migration barrier in bulk, we have simulated a 4*4*4 supercell with periodic boundary conditions in all three directions containing 511 atoms and one vacancy. None of the Si atoms are fixed and we let the system to get relaxed during the hop. The energy barrier obtained from the NEB method is about 0.402 eV (Figure 10). If we fix all other atoms to avoid rotation and translation in all directions, we get a higher energy barrier of 1.2 eV. However, this energy barrier is overestimated cause when an atom hops to the vacancy it can pushes the other atoms away and therefore the energy barrier might be smaller. The Vacancy migration barrier that we got with this method is comparable with the energy barrier from the literature (Table II). Then we will use this barrier for 3-dimensional vacancy diffusion simulations which has been explained in the next section.
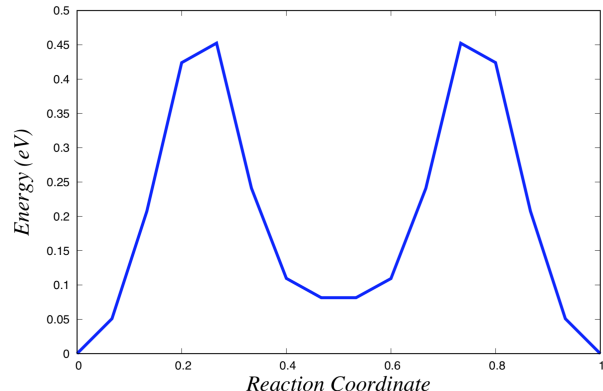

FIG. 10. Climbing image nudged elastic band data for silicon vacancy migration in bulk.

Method	Vacancy Migration Barrier (eV)
NEB	0.402
MD[10]	0.43
CP[11]	0.3
DFT[12]	0.4
Experiment[13]	0.5

TABLE II. Vacancy migration barrier for Silicon in bulk. The data labeled by NEB is the result from this work

To incorporate surface effects for 3D growth simulations for FCC silicon structure, further NEB calculations

is needed. As alluded to earlier, in this study, we restrict our attention to monitoring the diffusion of a single vacancy. We first discuss results for a single vacancy migration in bulk. However, to incorporate surface effects, it might be possible that two or more vacancies exist adjacent to the atom that is hopping. Therefore, we did a set of NEB calculations for a silicon atom hop where there are two or more vacancies exist. To simplify the problem, we only consider first nearest neighbors (Fig. 11). Therefore, there are 16 possibilities. Then NEB calculation is carried out to obtain the energy barriers. In these simulations, we fixed all the other atoms and move just one atom from initial position to the final position as you can see in Fig. 11a. The energy barriers are tabulated in table III. The first row in table III refers to figure 11a where the hopping atom has 3 nearest neighbors and the vacancy has 4 nearest neighbors (3*4). While after the migration the vacancy has 4 nearest neighbors and that atom has 3 nearest neighbors (4*3).

	Initial config.	Final config.	EBF	EBR
1	3*4	4*3	0.9027	0.9027
2	2*4	3*3	2.1683	0
3	1*4	2*3	4.3366	0
4	0*4	1*3	6.5049	0
5	3*3	4*2	0	2.1683
6	2*3	3*2	0.5325	0.5325
7	1*3	2*2	2.1683	0
8	0*3	1*2	4.3366	0
9	3*2	4*1	0	4.3366
10	2*2	3*1	0	2.1683
11	1*2	2*1	0.2409	0.2409
12	0*2	1*1	2.1683	0
13	3*1	4*0	0	6.5049
14	2*1	3*0	0	4.3366
15	1*1	2*0	0	2.1683
16	0*1	1*0	0	0

TABLE III. migration barriers for a silicon atom hop with only taking first nearest neighbors into account. EBF stands for forward energy barrier and EBR stands for reverse energy barrier.
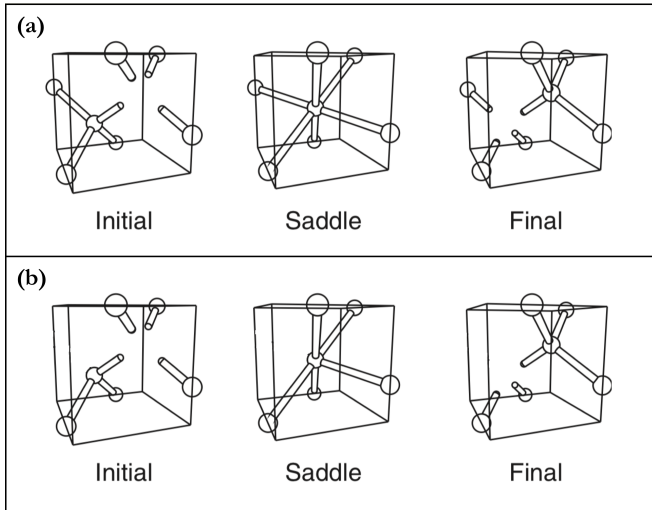

FIG. 11. Migration path of a single silicon atom hop. (a) refers to the first row of Table III and (b) refers to the second row

B. Lattice Metropolis Monte Carlo

1. Theory of Metropolis Monte Carlo

Metropolis Monte Carlo method[14] is a method that is used to sample the configuration space to compute certain quantities. For example, the expectation value of a quantity $A(r_1, r_2, ..., r_n)$ is given by

$$\langle A \rangle = \int \frac{1}{Z} A(r_1, r_2, ..., r_n) exp\left(\frac{-E(r_1, r_2, ..., r_n)}{k_b T} \right) dr_1 dr_2 ... dr_n \quad (3)$$

To uniformly sample the configuration space is computationally prohibitive for higher dimension configuration spaces. Hence, in Metropolis Monte Carlo, an importance sampling scheme is employed i.e. more probable samples (by the Boltzmann Distribution) are picked more frequently by using a suitable random walk in the configuration space.

The random walk algorithm is as follows:

- From a configuration a with energy E_a, pick a new configuration b with energy E_b.

- If $E_b < E_a$ unequivocally accept the new configuration for sampling, else accept with a probability of $exp\left(\frac{(E_a - E_b)}{k_b T} \right)$

Also, a requirement of the random walk is *detailed balance*. *Detailed balance* mandates that after considerable time steps the following should hold.

$$W(a \rightarrow b)P(a) = W(b \rightarrow a)P(b) \quad (4)$$

where $P(a)$ probability of state a and $W(a \rightarrow b)$ is probability of transition from state a to state b. It can be trivially shown that the above the above scheme honors equation 4.

2. Simulation Example: Equilibrium Structure of Ga-As

To test the method, we have demonstrated the formation of the equilibrium structure of Ga-As on a diamond structure lattice starting from a random initial distribution of Ge and As atoms. $E_a - E_b$ is computed from a difference in environments before and after a swap of the positions of two randomly picked atoms. Only the first nearest neighbours have been used to account for the

bonding environment. The bond strengths assumed for the calculation were Ga-Ga=0.3 eV, Ga-As=0.5 eV and As-As=0.1 eV. Details of the simulation are as follows:
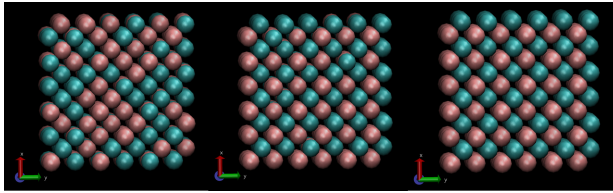

FIG. 12. Snapshots at three instances of the Ga-As (Ga:red; As:blue) Metropolis Monte Carlo as viewed from the [100] direction. a) Initial b) Intermediate c) End. Total number of atoms is 216.

- Orthonormal lattice vectors of lattice constant = 10.0 bohr (calculation indifferent to lattice constant) are used with each unit cell basis consisting of eight points corresponding to the usual FCC-diamond structure.

- The grid is built up by specifying N_x, N_y, N_z which are number of unit cells in each lattice direction making up total of $8 \times N_x \times N_y \times N_z$ lattice sites.

- Periodic boundary conditions are enforced on each direction.

- The atoms are initially seeded randomly with a 50-50 percent probability for each of the two species.

As seen in Fig 12, the arrangement of the Ga (red) and As (blue) atoms go from the initially random configuration to the zinc-blende which is typical of GaAs crystal. The result is also intuitive since formation of the Ga-As bond is most favourable given its large bond strength. Hence, in equilibrium, each atom sits at the centre of a tetrahedron with four atoms of the other species occupying the vertices of the tetrahedron.

To study the effect of temperature, the above simulation was repeated at three temperatures of 400 K, 600 K and 800 K. It was found that the energy of the 400 K case dropped quickly in the initial parts but later the drop was slower. On the other side of the spectrum, the 800 K dropped relatively slower than the 400 K case but retained the pace until the end. This can be rationalized by a couple of arguments. Lesser temperature aids to more often reject the positive energy difference jumps and hence has a higher rate of drop. However, lesser temperature also increases the possibility of getting temporarily stuck in a local minima of the configuration space. The plateaus in figure 13 for the T = 400 K and 600 K are clearly symptoms of this phenomenon. For the 800 K however, plateaus are relatively less pronounced since higher temperature prevents getting trapped in a local minima. Simulated annealing[15] and parallel tempering[16] are some ways to get around this problem for lower temperature simulations.
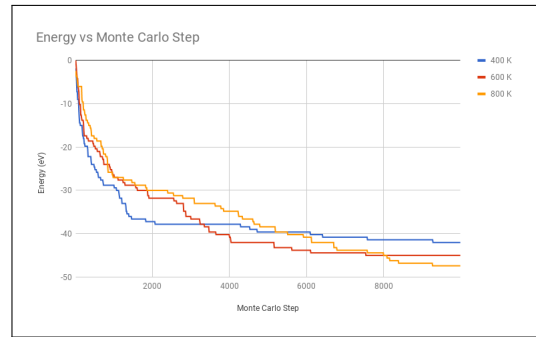

FIG. 13. Temperature dependence of Energy (eV) vs Timestep plot for the Metropolis algorithm for the 216 atom system. Energy is measured relative to the starting random configuration

The idea of the random walk getting stuck in the local minima of the configuration space was mentioned in the last paragraph. We now demonstrate this with an example. We consider a similar system as above albeit with very large number of atoms (8000 atoms) with temperature 800 K. Instead of starting from a random configuration, we start from a configuration (Figure 14.a where the atoms (red: Ga and blue: As) are separated. Figure 14.b represents the result of the random walk after 100 million MC steps. It is interesting to note that in spite of a fairly large number of steps, the equilibrium is not attained. To resolve this we, employ a simplified version of simulated annealing. In the first 6 million MC steps, we elevate the temperature to three times the desired temperature. And in the next 1 million MC, we slowly drop the temperature to the 800 K. With this exercise, the equilibrium structure is reached within 40 million MC steps. This effect is also amply evident in the figure 15 where annealing is shown to enable the system to reach a state of minimum energy.
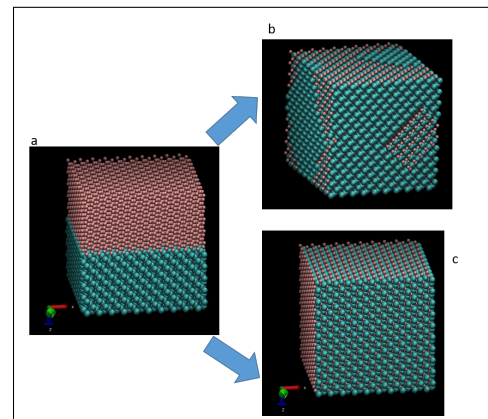

FIG. 14. Simulated Annealing Ga-As system containing 8000 atoms a) Starting configuration b) Without annealing at 100 million MC steps c) With annealing at 40 million MC steps

We now discuss some of the shortcomings of the model. Firstly the lattice MC will only work if the desired
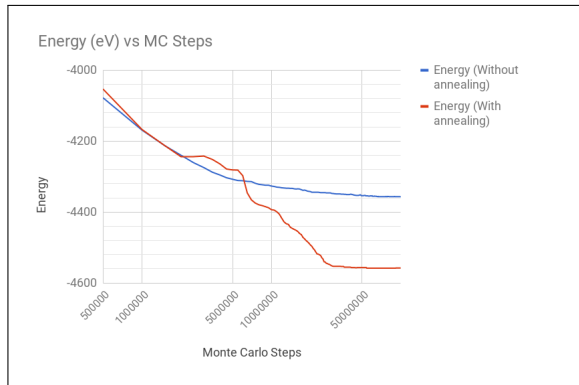
FIG. 15. Simulated Annealing: Plot of Energy (eV) vs MC Steps

equilibrium structure can be described by the limits of the configuration space spanned. For example, the above grid condition will make it impossible to predict a wurtzite structure since the initial grid does not allow it. We have used only first nearest neighbour interaction for simplicity. However, for better accuracy, one would have to use an atomic potential to evaluate the system energy before and after the proposed flip. Finally, one has use some additional conditioning such as parallel tempering or simulated annealing to ensure the random walk is effective.

C. Lattice Kinetic Monte Carlo

While the Metropolis algorithm described above is employed to study equilibrium structures or spanning the potential energy landscapes, the Kinetic Monte Carlo[17] is used to study dynamic processes like defect migration, phase transformation, etc. In this section, we will simulate vacancy hop using lattice Kinetic Monte Carlo.

1. Problem Description

We consider a periodic system of 1000 Si atoms in the usually diamond lattice structure. We introduce a vacancy by removing one atom. We generate the look up table for the applicable KMC processes. In this case, the only process is vacancy hop for which we already have a calculated migration energy of $E_a = 0.402$ eV. The objective is to retrieve back the activation barrier from the Mean Square Displacement of the vacancy. The simulation is run at 800 K , 1000 K, 1200 K and 1400 K. Periodic boundary conditions are applied.

2. Results

The diffusion hop process is carried out for the above temperatures and the MSD is recorded as a function of

time. A sample plot of the MSD vs time is shown in figure 16. At each time, the MSD will form a Gaussian about the mean. Hence, to reduce the scatter, we have computed the slope of the MSD as an average of 20 simulations for each temperature. This data is collated and the plot shown in figure 17. We get back a slope of $E_a = 0.32$ eV from the plot.
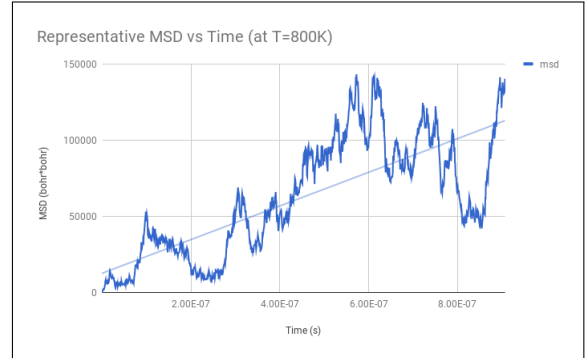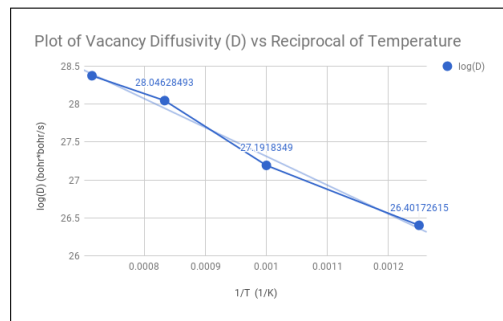

FIG. 16. Mean Square Displacement vs Time

FIG. 17. Vacancy Diffusivity vs Temperature^{-1}

IV. CONCLUDING REMARKS

Surface modification under different growth conditions was studied by computing the mean roughness during growth. Roughness evolution with temperature and time indicates the formation of smooth surfaces at higher temperatures where ad-atoms diffuse at a faster rate.

NEB calculations were carried out to obtain the energy barriers for silicon vacancy migration. First, vacancy migration in bulk was studied using SW potential for silicon. Thereafter, a single atom hop was studied with only taking first nearest neighbors into account. All in all there are 16 possibilities with one or more vacancies. The energy barriers will be then used for 3D Lattice Monte Carlo simulations.

In 3D Lattice Monte Carlo, the Metropolis algorithm was used to calculate the equilibrium structure of GaAs. Simulation annealing was demonstrated to prevent the random walk from being trapped in a local minima. The

problem of diffusion migration of Si vacancy in bulk was studied using Kinetic Lattice Monte Carlo.

This simulation only accounts for ad-atom addition and diffusion on the same layer. To accurately simulate real crystal growth, other phenomena such as long range diffusion, multi-step diffusion, atom desorption also need to be accounted for. Most importantly, this model is suitable to study structure whose phase stability is known. Since this assumes a rigid lattice model, it cannot capture temperature dependent crystal structure transformations. T capture those phenomena, one needs to include the possibility of additional lattice sites and calculate the relative probabilities of each possible Monte Carlo process. Further, kMC can be interfaced with atomic pair potentials to perform non-lattice simulations. If the crystal stability of a material is not known a priori, simulations should predict phase formation and stabilities.

V. CONTRIBUTIONS

All results in section II were obtained by Aditya. Writing and implementation of the kMC code, graphics generation and data analysis was entirely done using Mathematica 11.0. The bond energies for the nearest neighbour interactions were sourced from literature. The results in section III were obtained by Ramin. The simulations was entirely done using Lammps[9] and the figures were generated using gnuplot[18]. The results in section IV and V were obtained by Nelson. For the 3D calculations, the code was implemented in C++ and the graphics were generated using VMD[19].

[1] Manjusha Chugh and Madhav Ranganathan *Applied Surface Science* Volume **422**, 15 November 2017, Pages 1120-1128

[2] Manjusha Chugh and Madhav Ranganathan *Phys. Status Solidi C* **12**, No. 45, 408412 (2015)

[3] Dongwei Xu1, Peter Zapol, G. Brian Stephenson and Carol Thompson *The Journal of Chemical Physics* **146**, 144702 (2017);

[4] F. Nita, C. Mastail, and G. Abadias *PHYSICAL REVIEW B* **93**, 064107 (2016)

[5] Chen Zhou, Kun Zheng, Zhi-Ming Liao, Ping-Ping Chen, Wei Lu d and Jin Zou *J. Mater. Chem. C*, 2017, **5**, 5257-5262

[6] Kristofer Reyes, Peter Smereka, Denis Nothern, Joanna Mirecki Millunchick, Sergio Bietti, Claudio Somaschini, Stefano Sanguinetti and Cesare Frigeri *PHYSICAL REVIEW B* **87**, 165406 (2013)

[7] Wenliang Wang, Haiyan Wang, Weijia Yang, Yunnong Zhu and Guoqiang Li *Scientific Reports* volume **6**, Article number: 24448 (2016)

[8] Sebastian Tamariz, Denis Martin and Nicolas Grandjean Journal of Crystal Growth Volume **476**, 15 October 2017, Pages 58-63

[9] J Comp Phys, 117, 1-19 (1995).

[10] G.H. Gilmer et al. /Nucl. Instr. and Meth. in Phys. Res. B 102 (1995) 247-255

[11] P.E. Blochl et al., Phys. Rev. Lett. 70 (1993) 2435

[12] Fedwa El-Mellouhi et al. PHYSICAL REVIEW B 70, 205202 (2004)

[13] P G Coleman 2011 J. Phys.: Conf. Ser. 265 012001

[14] W. K. Hastings Biometrika, Volume 57 , Issue 1, 1 April 1970

[15] van Laarhoven, Peter J. M., Simulated Annealing: Theory and Applications 1987

[16] Earl, David J. and Deem, Michael W., Phys. Chem. Chem. Phys, 2005 vol7, issue 23.

[17] Voter, Arthur F., Radiation Effects in Solids, Springer Netherlands 2007

[18] T. Williams, C. Kelley, Gnuplot 4.6: an interactive plotting program, 2013

[19] Humphrey, W., Dalke, A. and Schulten, K., "VMD - Visual Molecular Dynamics", J. Molec. Graphics, 1996, vol. 14, pp. 33-38.